

## Cation mixing in natural $\text{MgAl}_2\text{O}_4$ spinel: A high-temperature $^{27}\text{Al}$ NMR study

HIDEKI MAEKAWA,\* SATOSHI KATO,† KATSUYUKI KAWAMURA,‡ AND TOSHIO YOKOKAWA

Division of Chemistry, Graduate School of Science, Hokkaido University Sapporo, 060, Japan

### ABSTRACT

The positional disorder of  $\text{Mg}^{2+}$  and  $\text{Al}^{3+}$  cations between the tetrahedral and octahedral sites in natural  $\text{MgAl}_2\text{O}_4$  spinel has been investigated by  $^{27}\text{Al}$  MAS NMR at room temperature and in-situ high-temperature  $^{27}\text{Al}$  NMR spectroscopy up to 1600 °C. The inversion parameter describing the disorder,  $x$ , where  $x$  stands for the positional disorder between Mg and Al cations in  $\text{Mg}_{1-x}\text{Al}_x(\text{Mg}_x\text{Al}_{2-x})\text{O}_4$ , increased with temperature. Below 1100 °C the inversion parameter,  $x$ , can be determined from MAS NMR measurements of quenched samples at room temperature. Above 1100 °C,  $x$  was estimated from the peak position in the high-temperature  $^{27}\text{Al}$  NMR spectra up to 1600 °C. The observed dependence of  $x$  with temperature was fitted using the model of O'Neill and Navrotsky (1983). The coefficients of the model obtained are  $\alpha = 35 \pm 5$  kJ and  $\beta = -32 \pm 5$  kJ, which are approximately equal in magnitude and opposite in sign. The  $x$  values observed in the present investigation are in agreement with the model. However the introduction of an additional entropy term,  $\Delta S_D$ , improved the fitting.  $\Delta S_D$  reduces the entropy of disorder relative to a random mixing model. This would reflect either a nonconfigurational entropy contribution or short-range Mg-Al order because of local charge balance. On the other hand, above 1400 °C a narrow peak appeared at about 60 ppm. This peak became narrower with increasing temperature up to 1600 °C. This behavior might suggest that a rapid exchange process among the fourfold-coordinated Al sites occurs in this temperature range.

### INTRODUCTION

Spinel is a mineralogical constituent of most igneous and metamorphic rocks. The ability of the spinel structure to incorporate many cation species of different valence states into its octahedral and tetrahedral sites lends stability to the spinel structure over a wide range of temperatures, pressures, and compositions. This adaptability has led to their utility as petrogenetic indicators of temperature and pressure (Buddington and Lindsley 1964; Sack 1982; Gasparik and Newton 1984; Jamieson and Roeder 1984; Mattioli and Wood 1988; Nell et al. 1989; Sack and Ghiorso 1991; Chamberlin et al. 1995). Spinel compounds have the general chemical formula  $(\text{A}_{1-x}\text{B}_x)\text{-}[\text{A}_x\text{B}_{2-x}]\text{O}_4$ , where parentheses represent fourfold-coordinated sites and brackets represent sixfold-coordinated sites, and  $x$  is referred to as the degree of inversion or the inversion parameter. Spinel compounds with  $x = 0$  are termed normal spinels, whereas those with  $x = 1$  are called inverse spinels. The relative size of the cations, Madelung energies calculated from the lattice energy, and

the ligand field stability for the transition metal cations determine the partitioning of cations in spinel.

The systematics of the spinel structure have been reviewed by Hill et al. (1979), and there have been many investigations of the relationship between the temperature and pressure on the cation distribution. Despite their simple structure, many spinels exhibit complex disordering phenomena involving the mixing of cations on two sites, which give rise to important consequences both for their thermodynamic and their physical properties.

Hafner and Laves (1961) first reported the cation distribution in an ordinary spinel ( $\text{MgAl}_2\text{O}_4$ ) determined by means of IR spectroscopy. The peak position of the spectrum shifted to a lower energy between 800 and 900 °C, which suggested an exchange of Mg and Al atoms. Brun and Hafner (1962) investigated this by means of  $^{27}\text{Al}$  NMR spectroscopy for a single-crystal sample. The NMR intensities depended on the direction of the applied magnetic field relative to the direction of the crystal lattice vector. With increasing temperature above 800 °C, the intensity of the NMR spectrum decreased considerably.

Yamanaka and Takéuchi (1983) undertook in-situ X-ray measurements on a synthetic spinel sample from 900 to 1800 °C. The similarity of the atomic scattering factors for Al and Mg made it difficult to determine their occupancy in the fourfold- and sixfold-coordinated sites. However, the  $x$  values could be estimated from the relationships between  $x$  and the A-O and B-O bond distances

\* Present address: Department of Metallurgy, Graduate School of Engineering, Tohoku University, Sendai, 980-77, Japan.

† Present address: Showa Denko Co. Ltd., Ichihara, Chiba, Japan.

‡ Present address: Department of Earth and Planetary Sciences, Tokyo Institute of Technology, 2-12-1, Ookayama, Meguro-ku, Tokyo, 152, Japan.

using thermal expansion coefficients for MgO and Al<sub>2</sub>O<sub>3</sub>. The  $x$  values evaluated from the measured lattice constants varied by 15% from room temperature to 1660 °C.

Calorimetric measurements have also been carried out on spinels. Navrotsky and Kleppa (1967) measured the enthalpy variation of the cation exchange in MgAl<sub>2</sub>O<sub>4</sub> spinel using solution calorimetry. The measured enthalpy was 0.9 kcal/mol at 1000 °C for a sample heat-treated at 700 °C. Assuming 10% cation disorder in this temperature range, the overall enthalpy of the transition was estimated to be 9 kcal/mol. The first-order equation for the reaction  $A(B_2)O_4 = A_{1-x}B_x(A_xB_{2-x})O_4$  was calculated assuming an ideal solid solution for the sublattice. The enthalpy change for the disorder reaction,  $\Delta H_D$ , was found to be represented by the relation,  $-\Delta H_D/RT = \ln [x^2(1-x)^{-1}(2-x)^{-1}]$ . O'Neill and Navrotsky (1983) suggested that the quadratic equation  $\Delta H_D = \alpha x + \beta x^2$  better represented the above exchange.

Recently, Peterson et al. (1991) conducted neutron diffraction measurements from 20 to 1000 °C. Their  $x$  values ranged within 0.31–0.33 at 900 °C. Millard et al. (1992) measured the <sup>27</sup>Al and <sup>17</sup>O NMR spectra for a quenched synthetic MgAl<sub>2</sub>O<sub>4</sub> spinel. The measured  $x$  values increased from  $x = 0.22$  at 700 °C to  $x = 0.29$  at 1000 °C. However, each of the measurements (HT neutron diffraction, <sup>27</sup>Al and <sup>17</sup>O NMR) showed a different temperature variation for  $x$ .

NMR measurements offer a direct method to determine the extent of the cation mixing; however, above 1000 °C, no NMR data could be obtained owing to problems related to quenching in the high-temperature cation disordering. In the present investigation, high-temperature measurements were undertaken for a natural spinel sample up to 1600 °C. A comparison was made of the high-speed magic-angle-spinning (MAS) NMR spectra with line shape simulation. The temperature dependence of the inversion parameter was estimated up to 1600 °C.

### EXPERIMENTAL METHODS

The natural spinel sample used in the present investigation is a pink specimen from Pamil. X-ray diffraction measurements were made with a Rigaku RINT-2000 X-ray diffractometer. The composition of the sample was determined by electron probe microanalysis (EPMA). The Mg to Al ratio obtained was Mg:Al = 0.99(1):2.00(1). Small amounts of Fe were also found, the concentration being 0.004 per four O atoms. High-temperature <sup>27</sup>Al NMR measurements were made using a home-built high-temperature static probe (Maekawa et al. 1997) with a Bruker MSL-200 spectrometer operated at 52.148 MHz for the <sup>27</sup>Al nucleus at temperatures up to 1600 °C. The spinel sample was placed into a cylindrical tube made of silica or boron nitride, which had both ends closed with silica wool. The sample holder was placed in a detection coil made of molybdenum wire turned six times. The temperature of the sample was monitored with an optical pyrometer (IR-FB, Chino Co., Ltd.). The accuracy of the measured temperature was ±1% for each temperature.

For the room temperature measurements, spinel samples were enclosed in platinum capsules (5 mm i.d.) and heated at 700, 800, 900, 1000, or 1100 °C in a SiC furnace and then drop quenched into water. The quenching time was estimated to be 0.2 s. MAS NMR signals of the quenched samples were observed with a Bruker MSL-300 spectrometer operated at 78.205 MHz with a Bruker high-speed MAS probe operated at a spinning speed of 14–15 kHz. A 1 M Al(NO<sub>3</sub>)<sub>3</sub> aqueous solution, whose chemical shift was set at zero, was utilized for the chemical shift reference. A pulse width of 0.6 μs was used for data acquisition for the solid samples with a 10 s delay for each data acquisition. An appropriate output power for the excitation pulse was set using an attenuator, where the  $\pi/2$  pulse of the solution <sup>27</sup>Al NMR signal was set at 14 μs. This condition corresponding to a  $\pi/16$  pulse for a 0.6 μs excitation pulse was used for the solid. Under these conditions, all of the central transitions are equally excited regardless of the magnitude of the nuclear quadrupole coupling constant (Millard et al. 1992). In the line shape simulation, the side-band intensities of the external transitions as well as the second-order nuclear-quadrupole interaction on the central transition of the MAS NMR line shape were taken into account. The line shape simulations were performed by means of the program Winfit (Massiot 1992). This program includes line shape simulations of the first-order contribution of the nuclear-quadrupole interactions to the side band intensities of the MAS NMR line shape as well as second-order contribution to the central components. The second-order nuclear quadrupole interaction causes a shift of the NMR frequency. The magnitude of the shift is a function of the nuclear-quadrupole coupling constant ( $\nu_Q$ ), its asymmetry ( $\eta$ ), the Larmor frequency ( $\nu_L$ ), and the angle between the principal axis of the electric-field-gradient (EFG) tensor and the applied magnetic field (Kundla et al. 1981). The MAS-NMR spectrum for the powdered sample can be calculated by a numerical integration of the function. The isotropic chemical shift is located at the left side shoulder of the central components and can be obtained from line shape simulation. The relative amounts of the individual species contributing to the <sup>27</sup>Al NMR peaks can be directly obtained from the peak area of the central components.

### RESULTS

#### Lattice constants and stoichiometry of the natural MgAl<sub>2</sub>O<sub>4</sub> spinel

X-ray diffraction measurement of the natural MgAl<sub>2</sub>O<sub>4</sub> spinel yielded a lattice parameter of  $8.0836 \pm 0.0005$  Å, which is in good agreement with the value obtained in previous investigations (8.083–8.084 Å). In the case of  $xAl_2O_3 - (1-x)MgAl_2O_4$  solid solutions, Navrotsky et al. (1986) found that the lattice constant decreases as  $x$  increases, i.e.,  $a = 8.0844(3)$ ,  $8.0684(2)$ , and  $8.0490(4)$  Å for  $x = 0, 0.1$ , and  $0.2$ , respectively. Consequently, our result suggests ideal stoichiometry for the MgAl<sub>2</sub>O<sub>4</sub> sample. X-ray diffraction refinements of the lattice constants

for quenched samples showed no systematic change within 0.001 Å for different heating conditions. The lattice parameters were not sensitive to the order-disorder of the cations in the quenched spinel samples up to 1000 °C.

### The $^{27}\text{Al}$ MAS NMR spectra of the heat-treated $\text{MgAl}_2\text{O}_4$ spinel

The  $^{27}\text{Al}$  MAS NMR spectra for the sample quenched from 700 °C at different heating periods are shown in Figure 1. The room temperature  $^{27}\text{Al}$  MAS NMR spectrum for the untreated sample contains a main doublet peak at about 0 ppm and a small high-frequency peak at about 70 ppm, corresponding to  $\text{AlO}_6$  octahedra ( $^{61}\text{Al}$ ) and  $\text{AlO}_4$  tetrahedra ( $^{41}\text{Al}$ ), respectively. The spectra are consistent with those of previous workers (Gobbi et al. 1985; Dupree et al. 1986; Wood et al. 1986; Millard et al. 1992). The intensity of the  $^{41}\text{Al}$  peak increased with the heat treatment time, suggesting that the cation disorder is time dependent. The line shape of the  $^{61}\text{Al}$  peak also changed with reaction period. With increasing duration of heat treatment, a broadening occurred on the right-hand side of the profile for the  $^{61}\text{Al}$  peak. This broadening suggests that the coordination environment of  $^{61}\text{Al}$  changes with increasing cation disorder over the reaction period. However, the left side of the  $^{61}\text{Al}$  peak showed little change. Because  $^{27}\text{Al}$  is a quadrupole nucleus, its line shape is influenced by the second-order nuclear-quadrupole interactions. The main doublet, which appeared at about 0 ppm, has the characteristic line shape of a second-order nuclear-quadrupole interaction. (Lippmaa et al. 1986) Further analysis requires computer simulation of the spectrum, including the first-order contribution to the spinning side bands, as well as the contribution of the second-order interaction to the central component. The  $^{27}\text{Al}$  spectra for heat-treated sample seem to tail off toward higher frequency sides. This observation suggests the presence of a distribution of  $\nu_Q$  values. Because the second-order nuclear-quadrupole interaction causes a shift toward the lower frequency side relative to the isotropic chemical shift position in the MAS NMR spectrum, the effect of the spectra of superposition of different  $\nu_Q$  values is significant on the lower frequency side, whereas the effect is minimal on the higher frequency side. A Gaussian distribution of  $\nu_Q$  values has been used for the simulation of the spectra in addition to exponential line broadening. The line shape simulations for the MAS NMR spectra are shown in Figure 1, and the calculated parameters are listed in Table 1. The spectra are well simulated. For the untreated sample, the main  $^{61}\text{Al}$  peak yields  $\nu_Q = 3.73$  MHz. This value is in good agreement with single-crystal NQR measurements (3.68 MHz, Brun and Hafner 1962). On the other hand, the long, low-frequency tail of the line shape for the heat-treated sample suggests the presence of a broad distribution of  $\nu_Q$  and  $\eta$  values for  $^{61}\text{Al}$  environments. The  $^{61}\text{Al}$  peak was well simulated with two components,  $^{61}\text{Al}(1)$  and  $^{61}\text{Al}(2)$ . The  $^{61}\text{Al}(1)$  component corresponds to the  $^{61}\text{Al}$  initially present in the untreated sample, which is

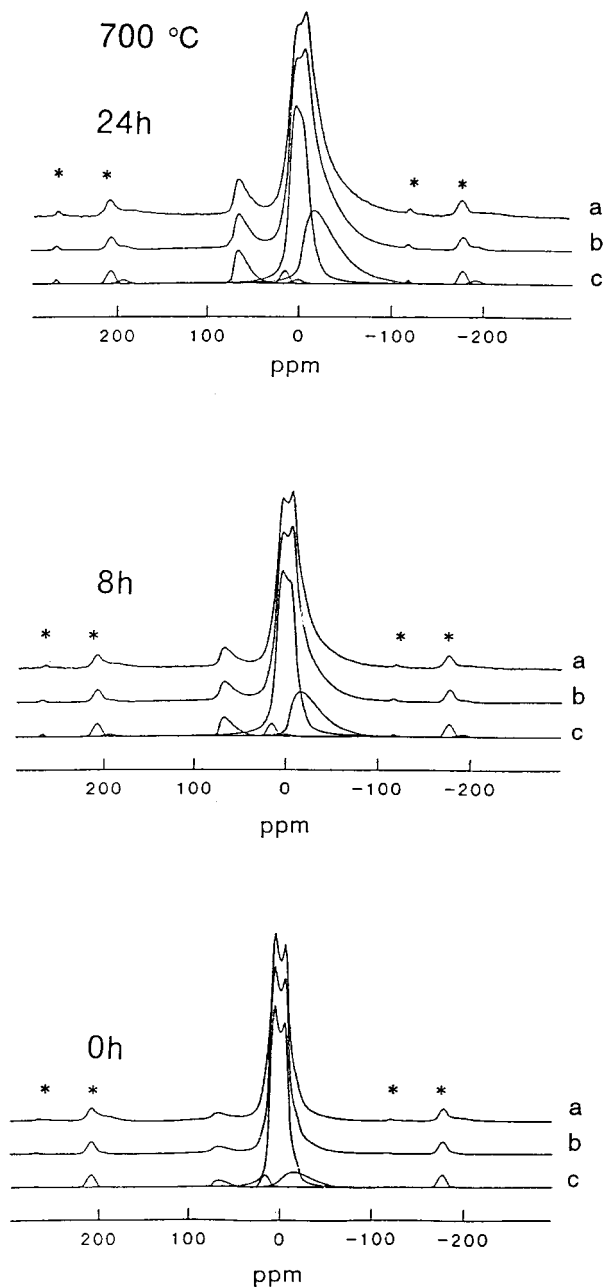


**FIGURE 1.** The dependence of the  $^{27}\text{Al}$  MAS NMR spectra for the sample quenched from 700 °C on the heat treatment time measured at magnetic field strength of 7 T; number of scans = 1000; spectrum window = 1 MHz; spinning speed = 15 kHz. (a) Observed spectrum; (b) simulated spectrum; (c) components of each of the simulated spectra whose parameters are shown in Table 1; \* = spinning side bands.

expected to have a narrower distribution of  $\nu_Q$  and  $\eta$  values, whereas  $^{61}\text{Al}(2)$  has a broader distribution. The asymmetric line shape for the  $^{61}\text{Al}$  peak is well simulated by these two components as shown in Figure 1. However in this simulation, only the distribution of  $\nu_Q$  was consid-

**TABLE 1.** The  $^{27}\text{Al}$  NMR parameters obtained from the line shape simulations shown in Figure 1

Site	$\nu_Q$ (MHz) ( $\pm 0.1$ )	$\eta$ ( $\pm 0.1$ )	$\delta_i$ (ppm) ( $\pm 1$ )	$\sigma$ (MHz) ( $\pm 0.2$ )	Intensity (%) ( $\pm 1$ )
$t = 0$ h					
$^{41}\text{Al}$	3.2	0.50	76.5	0.7	2.64
$^{61}\text{Al}(1)$	3.73	0.26	14.5	0.0	84.3
$^{61}\text{Al}(2)$	4.46	0.4	-1.0	0.8	13.0
$t = 8$ h					
$^{41}\text{Al}$	3.2	0.30	74.5	0.7	6.79
$^{61}\text{Al}(1)$	3.70	0.26	14.0	0.1	76.6
$^{61}\text{Al}(2)$	4.46	0.4	-1.0	1.0	16.6
$t = 24$ h					
$^{41}\text{Al}$	3.2	0.30	73.5	0.7	7.25
$^{61}\text{Al}(1)$	3.70	0.24	14.0	0.3	53.3
$^{61}\text{Al}(2)$	4.58	0.4	-1.0	1.2	39.5

Notes:  $\nu_Q$  = nuclear quadrupole coupling constant;  $\eta$  = asymmetry of electric field gradient tensor;  $\delta_i$  = isotropic chemical shift;  $\sigma$  = gaussian distribution width of  $\nu_Q$ .

ered. The distribution of  $\eta$  was not considered because of a limitation of the program used for the line-shape simulation. A further analysis would be necessary to determine whether or not a fit with a single peak is possible when considering the distribution of  $\eta$  in addition to  $\nu_Q$ .

The amounts of  $^{41}\text{Al}$  and  $^{61}\text{Al}$  sites in the sample were determined for each time period from the relative peak areas of the  $^{27}\text{Al}$  MAS NMR spectra. Figure 2 shows the heating-time dependence of the  $^{41}\text{Al}$  intensity for  $\text{MgAl}_2\text{O}_4$  spinel heat-treated at 700 °C. A heating-time dependence was observed at 700, 800, 900, 1000, and 1100 °C. At each temperature, the time evolution of the  $^{41}\text{Al}$  peak was well reproduced by an exponential fit (Kashii et al., in preparation):

$$[^{41}\text{Al}] = [^{41}\text{Al}_{\text{eq}}] \times \{1 - \exp[-k(t + t_0)]\} \quad (1)$$

where  $[^{41}\text{Al}_{\text{eq}}]$  represents the  $^{41}\text{Al}$  concentration at equilibrium and  $k$  is a rate constant. The  $x$  values at each temperature were obtained from the pre-exponential coefficients of the fitting functions.

### High-temperature NMR spectra of spinel single crystal

A high-temperature NMR measurement was made on a natural single-crystal  $\text{MgAl}_2\text{O}_4$  spinel. The temperature dependence of the  $^{27}\text{Al}$  NMR line shape is shown in Figure 3. The twofold axis [110] of the crystal is parallel to the applied magnetic field. Brun and Hafner (1962) reported that the resonance lines of the  $^{27}\text{Al}$  NMR depend on the applied magnetic field direction. They reported that when the threefold axis [111] is parallel to the applied magnetic field, the central transition from  $^{61}\text{Al}$  became a single line. This suggests that the principal axis of the EFG tensor of the  $^{27}\text{Al}$  nucleus lies along the same direction as the threefold axis. On the other hand, if the twofold axis is parallel to the applied magnetic field, four peaks from  $^{61}\text{Al}$  were observed. The  $^{41}\text{Al}$  peak was detected between these peaks, whose peak positions show no magnetic field direction dependence. The  $^{27}\text{Al}$  spectra

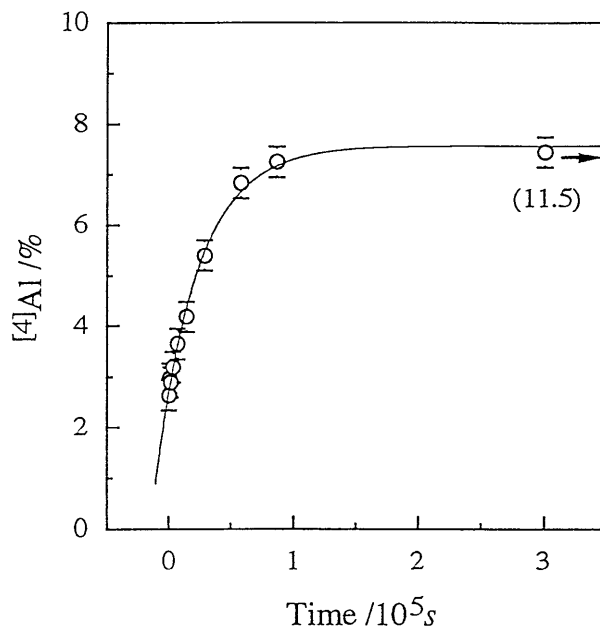


**FIGURE 2.** The dependence on the heat treatment time of the inversion parameter obtained from the peak area of  $^{27}\text{Al}$  MAS NMR spectra for samples quenched from 700 °C. The solid line represents a fit to the data with Equation 1, with  $[^{41}\text{Al}_{\text{eq}}] = 7.56\%$ ,  $k = 2.53 \times 10^5/\text{s}^1$ , and  $t_0 = 16700$  s. The data point obtained at  $t = 11.5 \times 10^5$  s is plotted at  $t = 3 \times 10^5$  s.

observed in the present investigation are consistent with those reported by Brun and Hafner (1962). However, no apparent  $^{41}\text{Al}$  peak was noticed. No significant change was observed in the spectra, from room temperature to

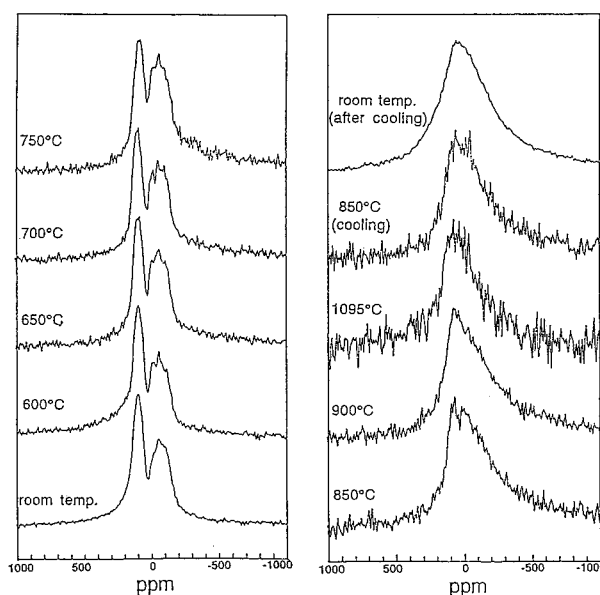


**FIGURE 3.** High-temperature in-situ static  $^{27}\text{Al}$  NMR spectra for a single-crystal spinel measured at magnetic field strength 4.7 T using a home-built high-temperature NMR probe.

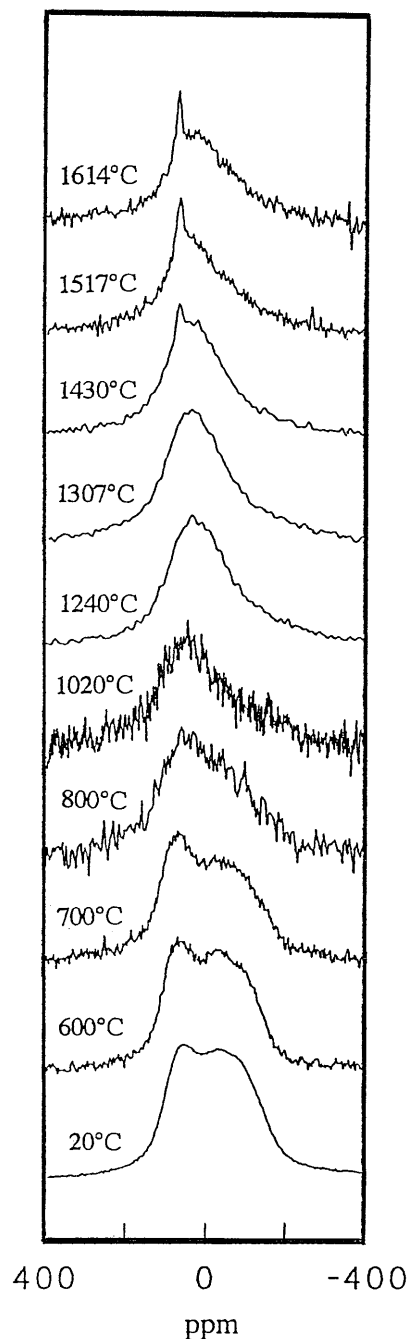


FIGURE 4. High-temperature in-situ static  $^{27}\text{Al}$  NMR spectra of a powdered natural spinel sample measured at magnetic field strength 4.7 T using a home-built high-temperature NMR probe.

750 °C. However, at temperatures above 850 °C, the spectrum became broad and featureless up to about 1100 °C. The room temperature  $^{27}\text{Al}$  NMR spectra for samples quenched after the high temperature measurements showed no significant change compared to those of the in-situ high-temperature spectra.

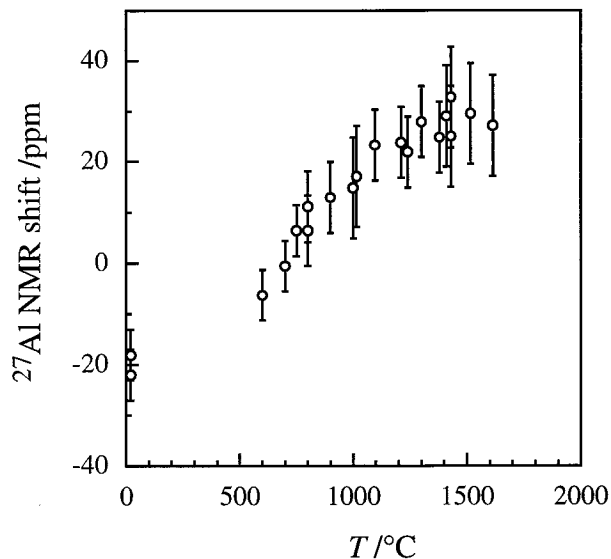


FIGURE 5. Temperature dependence of the center of gravity ( $\delta_{\text{CG}}$ ) of the high-temperature in-situ static  $^{27}\text{Al}$  NMR spectra of a natural spinel.

#### High-temperature $^{27}\text{Al}$ NMR spectra for powdered samples

The  $^{27}\text{Al}$  NMR spectra of powdered natural spinel samples at temperatures from room temperature up to 1600 °C are presented in Figure 4. Above 1400 °C, a sharp peak appears around 60 ppm. This peak became more intense with increasing temperature. A numerical integration of the powder spectrum from 400 to -400 ppm was calculated to obtain the center of gravity of the spectrum ( $\delta_{\text{CG}}$ ). The temperature dependence of  $\delta_{\text{CG}}$  is shown in Figure 5. The error bars for  $\delta_{\text{CG}}$  depend on the quality of the spectrum as well as on the base line distortion. The spectra at moderate temperature range (800–1100 °C) exhibited poor signal-to-noise ratios and distorted base lines, which lead to larger error bars ( $\pm 10$  ppm). A systematic increase in the  $\delta_{\text{CG}}$  value with temperature was observed.

## DISCUSSION

### Cation mixing below 1100 °C

The degree of cation exchange or  $x$  value below 1100 °C was determined from the ratio of the peak area for each of the  $^{47}\text{Al}$  and  $^{69}\text{Al}$  peaks. In Figure 6, the temperature dependence of  $x$  obtained during the present investigation, as well as those of other studies are compared. The  $x$  values herein are smaller than those obtained by Wood et al. (1986) and close to those obtained by Millard et al. (1992). Millard et al. (1992) suggested that the  $x$  values obtained by Wood et al. (1986) were overestimated because of the longer pulse width ( $\pi/6$ ) used in the acquisition of the NMR spectra. The relative peak intensities of different central lines in the MAS NMR spectra of quadrupole nuclei are dependent on pulse width (Lipp-

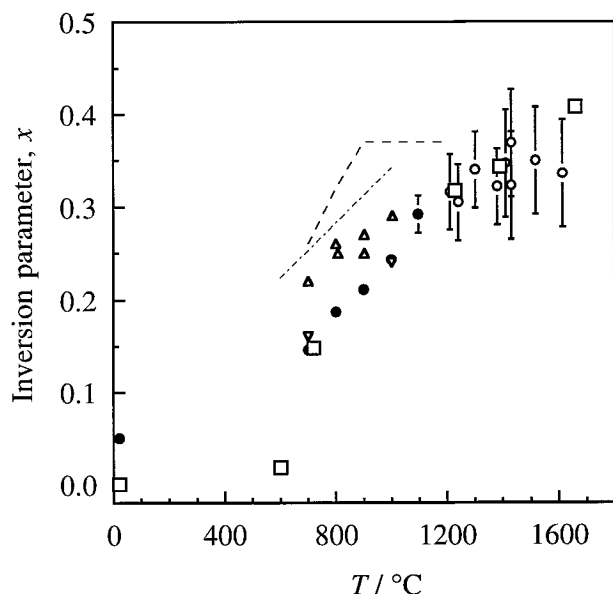


**FIGURE 6.** Temperature dependence of the inversion parameter,  $x$ , determined from the present investigation and that of previous investigations. Solid circles represent data from room temperature  $^{27}\text{Al}$  MAS NMR measurements of quenched samples in this study. Open circles are estimated data from high-temperature in-situ  $^{27}\text{Al}$  MAS NMR peak positions using the relationships shown in Figures 5 and 7. Triangles are  $^{27}\text{Al}$  and inverted triangles are  $^{17}\text{O}$  MAS NMR measurements for quenched synthetic samples by Millard et al. (1992). Dashed line represents  $^{27}\text{Al}$  MAS NMR measurements for quenched synthetic samples by Wood et al. (1986); dashed-and-dotted line represents high-temperature neutron diffraction measurements by Peterson et al. (1991) on the samples of Wood et al. (1986). Open boxes are the inversion parameter estimated from high-temperature X-ray data by Yamanaka and Takéuchi (1993) scaled to the present data (see text).

maa et al. 1986). The recommended data acquisition condition suggested by Millard et al. (1992), a magnetization tip angle of  $\pi/16$ , was used in the present investigation.

In the present investigation, as described above, the  $x$  values were obtained as coefficients used in the exponential fitting to the heating time dependence of the NMR intensities for  $^{41}\text{Al}$  at each temperature. The  $x$  values of the present data are slightly smaller than those obtained previously by Millard et al. (1992) from  $^{27}\text{Al}$  NMR but are similar to those obtained from  $^{17}\text{O}$  NMR.

#### Cation exchange above 1100 °C

There are only limited investigations of the cation exchange in spinels above 1100 °C because the samples quenched from such methods may have failed to attain thermodynamic equilibrium. Although the broad and featureless line shape of the  $^{27}\text{Al}$  static NMR spectra does not permit a direct determination of the inversion parameter from the relative peak area of each of the  $^{41}\text{Al}$  and  $^{61}\text{Al}$  components, the temperature change of the center of gravity of the  $^{27}\text{Al}$  spectra,  $\delta_{\text{CG}}$ , could provide an esti-

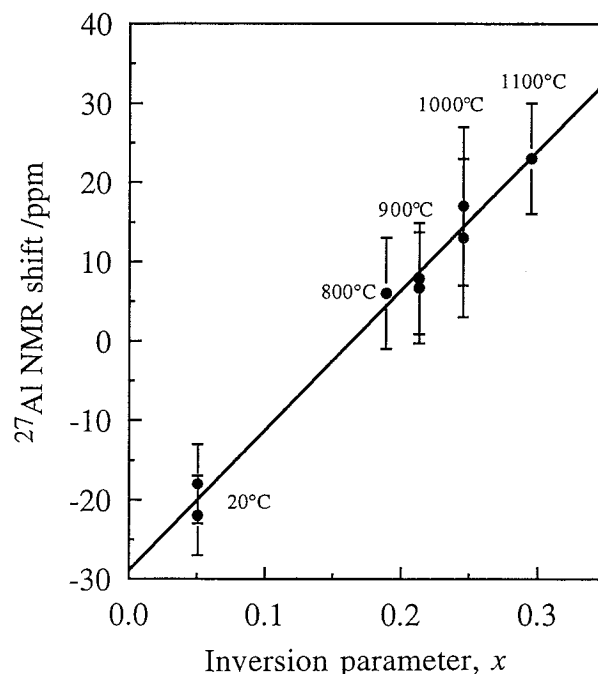


**FIGURE 7.** Relationship between the inversion parameter ( $x$ ) obtained from the room-temperature MAS NMR measurements and the center of gravity ( $\delta_{\text{CG}}$ ) of the high-temperature in-situ  $^{27}\text{Al}$  NMR spectra.

mation of the inversion parameter for samples above 1100 °C. Figure 5 shows the temperature dependence of  $\delta_{\text{CG}}$  of the high-temperature  $^{27}\text{Al}$  NMR peak obtained from in-situ high-temperature measurements. As can be seen in the figure,  $\delta_{\text{CG}}$  increases with increasing temperature. Figure 7 shows the relationship between the inversion parameter obtained from the room-temperature MAS NMR measurements and  $\delta_{\text{CG}}$  from the high-temperature spectra for the same temperatures. A nearly linear relationship was found between the inversion parameter and  $\delta_{\text{CG}}$ . With extrapolation of the relationship to higher temperatures, one can estimate the inversion parameter above 1100 °C using the  $\delta_{\text{CG}}$  value obtained from the high-temperature NMR spectra. The estimated inversion parameters are plotted in Figure 6 and listed in Table 2. In this treatment, the estimated inversion parameters contain errors contributed from several uncertain effects. Not only does  $\delta_{\text{CG}}$  depend on the proportion of  $^{41}\text{Al}$  and  $^{61}\text{Al}$  in the sample, which have different chemical shift values and lead to positive shifts of  $\delta_{\text{CG}}$  with increasing disorder, but it also depends on the change of  $\nu_{\text{Q}}$  and  $\eta$ , which are affected by changes of the local coordination environments of the Al atoms. Moreover, at temperatures above 1400 °C, an additional narrow peak appeared that would contain intensity from the external transitions. The addition of  $^{41}\text{Al}$  satellite intensity would lead to a systematic shift to higher frequency. All of these effects would contribute to the error of estimating  $x$  values, resulting in the relatively larger error bars at high temperature in Figure 6.

**TABLE 2.** Inversion parameter ( $x$ ) for  $\text{MgAl}_2\text{O}_4$  spinel obtained from MAS NMR measurements of quenched samples and from  $^{27}\text{Al}$  peak positions of high-temperature NMR spectra.

Temperature ( $^{\circ}\text{C}$ ) ( $\pm 5$ $^{\circ}\text{C}$ )	$x$ (MAS NMR)	$x$ (HT NMR)
20	0.050(15)	
700	0.146(15)	
800	0.187(15)	
900	0.211(15)	
1000	0.243(15)	
1096	0.292(20)	
1211		0.307(40)
1240		0.296(40)
1301		0.331(40)
1380		0.313(40)
1410		0.338(60)
1430		0.314(60)
1430		0.357(60)
1517		0.341(60)
1614		0.327(60)

The  $x$  values that can be compared with our present data at high temperatures were obtained from high-temperature X-ray measurements (Yamanaka and Takéuchi 1983). Their  $x$  values were estimated using the measured thermal expansion coefficients. The degree of disorder is small, with  $x = 0.057$  at  $720$   $^{\circ}\text{C}$  and  $x = 0.157$  at  $1660$   $^{\circ}\text{C}$ , compared to all the NMR measurements. However, if the X-ray derived data are scaled to fit the same  $x$  values of the present NMR data (by multiplying by a constant), then the X-ray data agree well with the trends of the present high-temperature NMR data as shown in Figure 6.

### Thermodynamic model

If we express the changes in enthalpy and volume upon disordering as  $\Delta H_D$  and  $\Delta V_D$ , and the change in the configurational and nonconfigurational entropy as  $\Delta S_C$  and  $\Delta S_D$ , then the change in the free energy upon disordering,  $\Delta G_D$ , is,

$$\Delta G_D = \Delta U_D - T(\Delta S_C + \Delta S_D) + P\Delta V_D, \quad (2)$$

where  $\Delta U_D$  is the internal energy change. At equilibrium,  $\partial\Delta G_D/\partial x = 0$ .

The thermodynamical model described by Navrotsky and Kleppa (1967) and O'Neill and Navrotsky (1983) assumed random cation mixing on the tetrahedral and octahedral sites. This yields an ideal configurational entropy given by,

$$\Delta S_C = -R\{x \ln x + (1-x)\ln(1-x) + x \ln(x/2) + (2-x)\ln[1-(x/2)]\}. \quad (3)$$

Differentiation of  $\Delta S_C$  with respect to  $x$  results in  $-R \ln [x^2(2-x)^{-1}(1-x)^{-1}]$ , which can be written as  $-R \ln K$ , where  $K$  is the equilibrium constant of cation mixing between tetrahedral and octahedral sites. Substituting Equation 3 into Equation 2, executing differentiation with respect to  $x$ , and neglecting the  $\Delta V_D$  term, one obtains,

$$\ln K = -(RT)^{-1}(\partial\Delta U_D/\partial x) + R^{-1}(\partial\Delta S_D/\partial x). \quad (4)$$

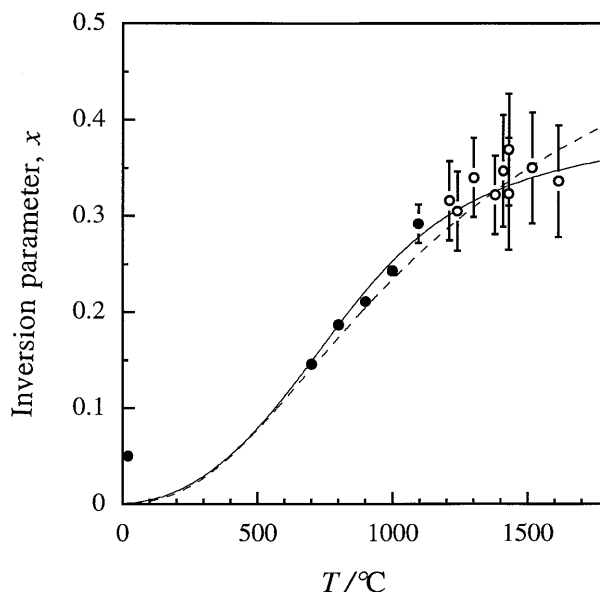


**FIGURE 8.** Temperature dependence of the inversion parameter,  $x$ , determined in the present investigation. Solid circles represent  $^{27}\text{Al}$  MAS NMR measurements of quenched samples in this study. Open circles are from high-temperature in-situ  $^{27}\text{Al}$  MAS NMR peak positions using the relationship shown in Figures 5 and 7. Solid line is best fit of the O'Neill and Navrotsky model;  $\ln K = -(\alpha + 2\beta x)/RT$  with  $\alpha = 35(\pm 5)$  kJ and  $\beta = -32(\pm 5)$  kJ. Dashed line is best fit of Equation 5 with  $\alpha = 30.5$  kJ,  $\beta = -30$  kJ, and  $\Delta S_D = -13$  J/K.

O'Neill and Navrotsky (1983) supposed a quadratic dependence of  $\Delta U_D$  on  $x$ , which can be written in the form  $\Delta U_D = \alpha x + \beta x^2$ , and neglected any nonconfigurational entropy contribution. This yields the equilibrium constant with a simpler equation,  $\ln K = -(\alpha + 2\beta x)/RT$ . The present data, when fitted with the O'Neill and Navrotsky model, give  $\alpha = 35(\pm 5)$  kJ and  $\beta = -32(\pm 5)$  kJ. O'Neill and Navrotsky (1983) calculated  $\alpha$  and  $\beta$  for various spinels from the variation of the inversion parameters. They found that the coefficients  $\alpha$  and  $\beta$  are approximately equal in magnitude and opposite in sign to each other for all spinels, which was predicted from their lattice energy model. Our  $\alpha$  and  $\beta$  values are also approximately equal in magnitude and opposite in sign. A line fitted to the present data is shown in Figure 8. The inversion parameter follows the trends predicted by the O'Neill and Navrotsky model.

On the other hand, the vibrational entropy,  $\Delta S_D$ , reflects the modified vibrational properties of spinel with different degrees of inversion. This term is usually regarded as subordinate in magnitude to the configurational term and was assumed to be zero by Navrotsky and Kleppa (1967) and O'Neill and Navrotsky (1983). However, if the inversion parameters obtained in the present investigation are fitted to a model adding a  $\Delta S_D$  term as,

$$\ln K = -(\alpha + 2\beta x)/RT + \partial(\Delta S_D/R)/\partial x, \quad (5)$$

yields  $\alpha = 30.5$  kJ,  $\beta = -30$  kJ, and  $\Delta S_D = -13$  J/K. A

fitted line is shown in Figure 8. Here,  $\Delta S_D$  represents the nonconfigurational entropy difference of completely normal,  $x = 0$ , and completely inverse,  $x = 1$ , spinel. Wood et al. (1986) suggested from the  $P$ - $T$  slope of the reaction enstatite + spinel = pyrope + forsterite, which strongly depends on the degree of cation mixing of the spinel, that the entropy of disorder calculated from the random mixing model overestimates the residual entropy of spinel derived from calorimetric measurements. The estimated residual entropy for spinel at about 900–1000 °C was 4 J/K, which is considerably smaller than that calculated from the configurational entropy from the random-mixing model. In the present experiment, the inversion parameter obtained at 1000 °C was  $x = 0.243$ , which gives a configurational entropy of 10.7 J/K assuming random mixing. The value obtained in the present investigation,  $\Delta S_D = -13$  J/K, reduces the entropy contribution at 1000 °C from 10.7 J/K for a random mixing model to 7.5 J/K, which is consistent with the trend expected by Wood et al. (1986). The reduction of the entropy of disorder from that calculated from the random mixing model would suggest either the existence of a nonconfigurational contribution to the entropy or short-range Mg-Al order in the spinel sublattice, which is expected to reduce the entropy of disorder considerably (Wood et al. 1986).

#### Possibility of a rapid exchange reaction among fourfold-coordinated sites above 1400 °C

The NMR spectrum above 1400 °C shows a sharp peak around 60 ppm. This chemical shift value corresponds to the  $^{41}\text{Al}$  species. There is a possibility that a small amount of impurity (e.g.,  $\text{B}_2\text{O}_3$  from the BN sample holder) exists in the natural spinel sample and might cause a partial melting of the phase and a sharpened NMR resonance line at high temperature. However, we believe that this peak suggests the occurrence of a rapid exchange reaction inside the spinel structure. Because the peak became more intense with increasing temperature and the resonance position appears at around that of the fourfold-coordinated Al species, we suggest that a rapid exchange reaction (on the order of  $10^5$  Hz) among the fourfold-coordinated sites in the spinel starts at these high temperatures.

#### ACKNOWLEDGMENTS

This work was supported by the Corning Research Foundation and a Grant-in-Aid for Scientific Research (no. 04554025) from the Ministry of Education, Science, Sports and Culture, Japan.

#### REFERENCES CITED

- Brun, E. and Hafner, S. (1962) Die elektrische Quadrupolspaltung von  $\text{Al}^{27}$  in Spinell  $\text{MgAl}_2\text{O}_4$  und Korund  $\text{Al}_2\text{O}_3$ . I. Paramagnetische Kernresonanz von  $\text{Al}^{27}$  und Kationenverteilung in Spinell. *Zeitschrift für Kristallographie*, 117, 37–62.
- Buddington, A.F. and Lindsley, D.H. (1964) Iron-titanium oxide minerals and synthetic equivalents. *Journal of Petrology*, 5, 310–357.
- Chamberlin, L., Beckett, J.R., and Stolper, E. (1995) Palladium oxide equilibration and the thermodynamic properties of  $\text{MgAl}_2\text{O}_4$  spinel. *American Mineralogist*, 80, 285–296.
- Dupree, R., Lewis, M.H., and Smith, M.E. (1986) A study of the vacancy distribution in non-stoichiometric spinels by magic-angle spinning NMR. *Philosophical Magazine A*, 53, L17–L20.
- Gasparik, T. and Newton, R.C. (1984) The reversed alumina contents of orthopyroxene in equilibrium with spinel and forsterite in the system  $\text{MgO}-\text{Al}_2\text{O}_3-\text{SiO}_2$ . *Contributions to Mineralogy and Petrology*, 85, 186–196.
- Gobbi, G.C., Christoffersen, R., Otten, M.T., Miner, B., Buseck, P.R., Kennedy, G.J., and Fyfe, C.A. (1985) Direct determination of cation disorder in  $\text{MgAl}_2\text{O}_4$  spinel by high-resolution  $^{27}\text{Al}$  magic-angle-spinning NMR spectroscopy. *Chemistry Letters*, 771–774.
- Hafner, S. and Laves, F. (1961) Ordnung/Unordnung und Ultrarotabsorption. III. Die Systeme  $\text{MgAl}_2\text{O}_4-\text{Al}_2\text{O}_3$  und  $\text{MgAl}_2\text{O}_4-\text{LiAl}_3\text{O}_8$ . *Zeitschrift für Kristallographie*, 115, 321–330.
- Hill, R.J., Craig, J.R., and Gibbs, G.V. (1979) Systematics of the spinel structure type. *Physics and Chemistry of Minerals*, 4, 317–339.
- Jamieson, H.E. and Roeder, P.L. (1984) The distribution of Mg and  $\text{Fe}^{2+}$  between olivine and spinel at 1300 °C. *American Mineralogist*, 69, 283–291.
- Kundla, E., Samoson, A., and Lippmaa, E. (1981) High-resolution NMR of quadrupolar nuclei in rotating solids. *Chemical Physics Letters* 83, 229–232.
- Lippmaa, E., Samoson, A., and Mägi, M. (1986) High-resolution  $^{27}\text{Al}$  NMR of aluminosilicates. *Journal of the American Chemical Society*, 108, 1730–1735.
- Maekawa, H., Nakao, T., Shimokawa, S., and Yokokawa, T. (1997) Coordination of sodium ions in  $\text{NaAlO}_2-\text{SiO}_2$  melts: A high temperature  $^{23}\text{Na}$  NMR study. *Physics and Chemistry of Minerals*, 24, 53–65.
- Massiot, D., Bessada, C., Coutures, J.P., and Taulelle, F. (1990) A quantitative study of  $^{27}\text{Al}$  MAS NMR in crystalline YAG. *Journal of Magnetic Resonance*, 90, 231–242.
- Mattioli, G.S. and Wood, B.J. (1988) Magnetite activities across the  $\text{MgAl}_2\text{O}_4-\text{Fe}_3\text{O}_4$  spinel join, with application to thermobarometric estimates of upper mantle oxygen fugacity. *Contributions to Mineralogy and Petrology*, 98, 148–162.
- Millard, R.L., Peterson, R.C., and Hunter, B.K. (1992) Temperature dependence of cation disorder in  $\text{MgAl}_2\text{O}_4$  spinel using  $^{27}\text{Al}$  and  $^{17}\text{O}$  magic-angle spinning NMR. *American Mineralogist*, 77, 44–52.
- Navrotsky, A. and Kleppa, O.J. (1967) The thermodynamics of cation distributions in simple spinels. *Journal of Inorganic and Nuclear Chemistry*, 29, 2701–2714.
- Navrotsky, A., Wechsler, B.A., Geisinger, K., and Seifert, F. (1986) Thermochemistry of  $\text{MgAl}_2\text{O}_4-\text{Al}_{8/3}\text{O}_4$  defect spinels. *Journal of the American Ceramic Society*, 69, 418–422.
- Nell, J., Wood, B.J., and Mason, T. (1989) High-temperature cation distributions in  $\text{Fe}_2\text{O}_3-\text{MgAl}_2\text{O}_4-\text{MgFe}_2\text{O}_4-\text{FeAl}_2\text{O}_4$  spinels from thermopower and conductivity measurements. *American Mineralogist*, 74, 339–351.
- O'Neill, H.S.C. and Navrotsky, A. (1983) Simple spinels: crystallographic parameters, cation radii, lattice energies, and cation distribution. *American Mineralogist*, 68, 181–194.
- Peterson, R.C., Lager, G.A., and Hitterman, R.L. (1991) A time-of-flight neutron powder diffraction study of  $\text{MgAl}_2\text{O}_4$  at temperatures up to 1273 K. *American Mineralogist*, 76, 1455–1458.
- Sack, R.O. (1982) Spinels as petrogenetic indicators: Activity-composition relations at low pressures. *Contributions to Mineralogy and Petrology*, 79, 169–186.
- Sack, R.O. and Ghiorso, M.S. (1991) Chromian spinels as petrogenetic indicators: Thermodynamics and petrological applications. *American Mineralogist*, 76, 827–847.
- Wood, B.J., Kirkpatrick, R.J., and Montez, B. (1986) Order-disorder phenomena in  $\text{MgAl}_2\text{O}_4$  spinel. *American Mineralogist*, 71, 999–1006.
- Yamanaka, T. and Takéuchi, Y. (1983) Order-disorder transition in  $\text{MgAl}_2\text{O}_4$  spinel at high temperatures up to 1700°C. *Zeitschrift für Kristallographie*, 165, 65–78.

MANUSCRIPT RECEIVED JULY 23, 1996

MANUSCRIPT ACCEPTED JULY 1, 1997